Progress In Electromagnetics Research B, Vol. 98, 87–105, 2023

A Miniaturized Antenna for Breast Cancer Detection at the 5.72–5.82 GHz ISM Band Based on the DGS Technique

Lala A. El Vadel[1, *], Dominic B. O. Konditi[2], and Franck Moukanda Mbango[3, 4]

Abstract—This paper presents an alternative solution for detecting breast cancer through planar antennas. The designed antenna electric parameters are the best gain for tiny radiation elements, along with the suitable characteristic impedance and bandwidth focusing on a specific application. Antennas are deployed nowadays to provide access to the detection of malignant tumors. That solution coexists with those in the hospitals (X-ray Mammography, Biopsy, Ultrasound, and Tomography), as breast cancer is a worldwide health concern because many women die yearly. Unfortunately, none of these methods are efficient as microwave imaging techniques. In terms of rapidity, efficiency, sensitivity, and accuracy, a small microstrip patch antenna operating at the Industrial, Scientific, Medical (ISM) band (5.72–5.82 GHz) is proposed in this paper for early breast tumor screening. Designed from the High-Frequency Structure Simulator (HFSS), the rectangular microstrip patch-antenna of $12 \times 12 \times 1\,\text{mm}^3$, etched on an FR4 HTG-175 dielectric material (relative permittivity of 4.4 and 0.02 of loss tangent) has been simulated, prototyped, and experimentally measured with ZVA50 Vector Network Analyzer (VNA). The defective ground structure technique has been used to achieve the goals of the final prototype. The proposed antenna has 51.22 dB of return loss, 230 MHz of bandwidth, with a radiation efficiency of 82% and a gain of 1.45 dBi at the resonance frequency of 5.73 GHz. Simulation results have been well-concluded through different tumor positions on the breast to take comprehensive precautions. Furthermore, a comparison with other antenna designs has been made. Due to the available laboratory equipment, the suggested work focused on the research part.

1. INTRODUCTION

According to World Health Organization (WHO), cancer is the second leading cause of death worldwide [1]. Malignant tumors are cancerous and can extend to other body parts. At the same time, when cancer spreads fully in any part of the body, it becomes difficult to save the patient's life. Hence, the need for early breast cancer detection is a necessity. Several early breast cancer (BC) detection methods have been developed, such as Biopsy, X-ray Mammography, Ultrasound, and Tomography [2]. Nowadays, Mammography is the gold standard for breast imaging. However, the National Cancer Institute advises women between 40 and 50 year ages to have Mammography twice a year. Above 50 years old, the screening must be performed annually [3]. However, this method has a false-negative rate of 4 to 34 percent [3]. In addition, the ionizing nature of X-rays raises the possibility of aggravating every cancer.

Consequently, microwave BC imaging techniques are being developed to provide a safer and more accurate method than Mammography [4]. The biopsy-based method effectively detects breast cancer

Received 10 January 2023, Accepted 3 February 2023, Scheduled 10 February 2023

* Corresponding author: Lala Aicha El Vadel (el.lalaaicha@students.jkuat.ac.ke).

[1] Department of Electrical Engineering, Pan African University Institute for Basic Sciences and Technology and Innovation, Nairobi, Kenya. [2] School of Electrical and Electronic Engineering, Faculty of Engineering and Built Environment, Technical University of Kenya (TU-K), Nairobi, Kenya. [3] Electrical and Electronics Engineering Laboratory, Marien Ngouabi University, BP: 69, Brazzaville, Congo. [4] Faculty of Sciences and Techniques, Marien Ngouabi University, BP: 69, Brazzaville, Congo.

cells' existence but is still limited. In addition, this method must be repeated severally when the collected sample tissue is insufficient. Such an approach can help to avoid problems, but it is painful, time-consuming, and expensive [5]. Other methods, such as ultrasound and MRI, have high false negative rates as drawbacks. A microwave system is an innovative, alternative, and flexible method to detect BC using an electromagnetic signal [4]. Water is critical in identifying tissue permittivity [6]. Soft water-containing tissue has a higher dielectric constant (permittivity) than the one having healthy tissue [3]. In addition, the tumor's electrical properties are 10% more than healthy tissues. Biological tissue is a highly non-homogeneous material. It is a mixture of physical components with different permittivities and conductivities, basically homogenous modeling at a particular frequency. The antenna acts as a sensor when the breast tissue is placed closely. Hence, the transmission and reflection coefficients can capture variations of the breast tissue electric property.

Microstrip patch antennas are widely used in breast cancer detection due to their ease of fabrication, robust design, low profile, and low cost [7]. An antenna with a wide rectangular slot on one substrate side and a substrate-forked microstrip feed on the other side is presented in [6]. The research in [4] suggests a low-cost textile wearable antenna for BC detection at 2.4 GHz for Industrial, Scientific, and Medical (ISM) applications. Wearable jeans is used as an insulator to design an antenna with a slot-loaded over a patch and a copper ground plane. The radiation element has not been tested. An ultra-wideband (UWB) flexible antenna, presented in [8], has been designed, and its performance was tested on a cubic breast phantom. Still, there were no investigations into the impact of the tumor within the breast phantom. Several studies have been done without validation in worse conditions, but some investigated the situation further. It is the case in [9] where the Breast Phantom tumor has been detected by using a microstrip patch antenna. Reference [10] designs an antenna array of eight antennas for a microwave breast imaging system. Each element is arranged circularly to face the breast phantom for better tumor detection directly. A UWB elliptical ring antenna with a humanoid cubic breast phantom was used to investigate the impact of the breast phantom's presence on the antenna's reflection coefficient [11]. An on-body microstrip antenna was developed in S-band varying from 1.5 to 3 GHz. A comparison between an antenna in free space and a cancer-affected breast model to diagnose breast cancer at the earliest stage is presented in [12]. Most of the cited references did not check the device's capability to detect tumors in different positions.

This paper presents a new small size ($12 \times 12 \times 1\,\mathrm{mm}^3$) antenna corresponding to the electrical size $0.228\lambda_0 \times 0.228\lambda_0 \times 0.019\lambda_0$. This microstrip antenna operates at the 5.72–5.82 GHz ISM band for breast cancer detection and uses the Microwave Imaging (MWI) technique. Designed from High-Frequency Structure Simulator (HFSS) before prototyping, the defective ground structure (DGS) technique was used for the proposed antenna to reduce its dimensions, which allowed achieving excellent electric characteristic (reflection coefficient, bandwidth, matching level, gain, and radiation pattern) parameters in the frequency range cited above. In addition, the prototype has been measured with VNAZVA50 for experimental validation. Three main sections are presented below, especially focusing on the method, results, discussion, and the comparative results with some recent studies. As seen in the literature, there is a large panel of techniques, and MWI and magnetic resonance imaging (MRI) are among them. MWI and MRI are painless imaging techniques. MWI uses a lower frequency than MRI, resulting in lower-resolution images than MRI. However, MWI can penetrate deeper into the tissue than MRI, allowing it to detect tumors or abnormalities that may not be visible on MRI. MWI is also said to be faster than MRI, and it does not require the patient to remain still for long periods. Furthermore, unlike MRI used only in hospitals, the MWI system can be used in ambulances. This makes MWI more accessible and convenient for certain patients and situations.

2. METHOD

The proposed antenna description is detailed through several subsections, used equations, and the prototype manufactured with an FR4 HTG-175 dielectric. This part presents a phantom breast design used for the approach validation.

2.1. Antenna Design

The proposed radiation element is a microstrip patch powered by a microstrip feedline, while the ground plane is partially degraded, as shown in Figure 1.

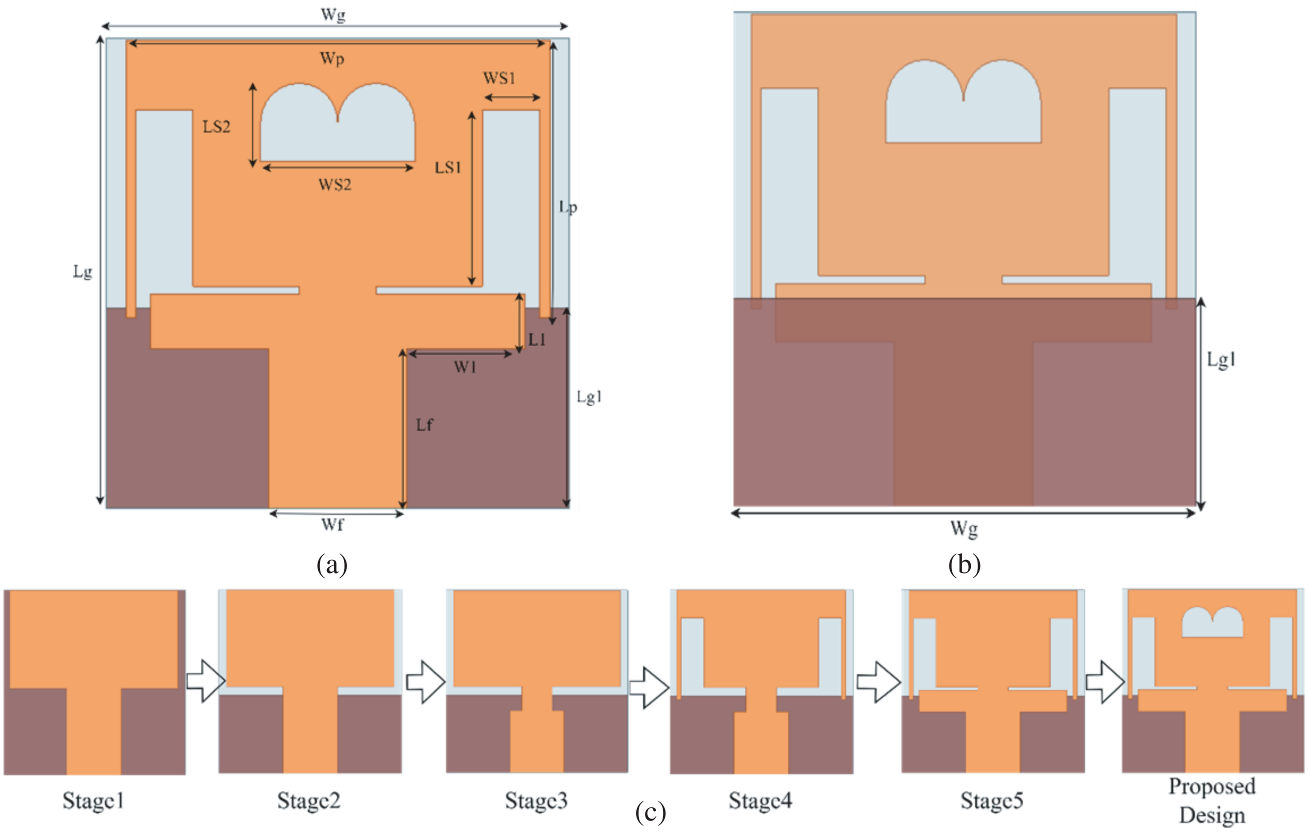

Figure 1. (a) Top view of the proposed antenna for breast cancer detection. (b) Bottom view of the proposed antenna for breast cancer detection. (c) Design stages.

2.2. Mathematical Model

Rectangular microstrip antenna dimensions are determined from empirical patch antenna equations. Eq. (1) gives the length L of the rectangular patch,

$$L = L_{eff} - 2\Delta l \tag{1}$$

where L_{eff} is the effective length and Δl the gap between both lengths. At the same time, Eq. (2) allows evaluating Δl as follows,

$$\Delta l = 0.412h \frac{(\varepsilon_r + 0.3)\left(\frac{W}{h} + 0.264\right)}{(\varepsilon_r - 0.258)\left(\frac{W}{h} + 0.8\right)} \tag{2}$$

with h being the dielectric thickness, W the patch width, and ε_r the material relative permittivity. Eqs. (3) and (4) give the rectangular patch width and effective dielectric permittivity, respectively [13],

$$W = \frac{c}{2f_0\sqrt{\frac{\varepsilon_r + 1}{2}}} \tag{3}$$

$$\varepsilon_{eff} = \frac{\varepsilon_r + 1}{2} + \frac{\varepsilon_r - 1}{2}\left(1 + \frac{12h}{W}\right)^{-1/2} \tag{4}$$

Table 1. Proposed antenna design parameters.

Parameter	Value (mm)	Description
Lg	12	Length of the substrate
Wg	12	Width of the substrate
$Lg1$	5.1	Length of the ground
Wg	12	Width of the ground
Lf	4.06	Length of the feedline
Wf	3.57	Width of the feedline
Lp	7.1	Length of the patch
Wp	11	Width of the patch
$LS1$	4.5	Length of the U-shaped slot
$WS1$	1.5	Width of the U-shaped slot
$LS2$	2	Length of the B-shaped slot
$WS2$	4	Width of the B-shaped slot
$L1$	3.06	Length of the Arm shaped slot
$W1$	1.4	Width of the Arm shaped slot

where f_0 is the operating frequency, c the speed of light in a vacuum, and ε_r the material's relative permittivity. As a result, the computed patch length is 15.95 mm, and the patch width is 12.22 mm. However, these theoretical values are insufficient to achieve the design's goal, which is a small-size miniaturized antenna. Table 1 presents the antenna's dimensions.

2.3. Design Evolution

The evolution stages of the antenna design are briefed in Figure 1(c). In stage 1, a simple rectangular patch antenna with a complete ground plane is selected with $12 \times 12\,\mathrm{mm}^2$. Moreover, a $50\,\Omega$ feedline powers the antenna. The radiation element ground plane is defective in stage 2 to improve its bandwidth. In stage 3, the feedline is reduced to shift the resonance frequency. In stages 4 and 5, two U-shaped cuts and arms slots were introduced, which further helped to lower the reflection coefficient to -38.48 dB. In the final stage of the proposed antenna, a B-shaped cut was made on the patch to improve the reflection coefficient and the bandwidth in the target ISM band. All stages of the proposed design were simulated through HFSS software.

2.4. Breast Phantom Designing

The human breast phantom comprises three layers: skin, fat, and glandular tissue. The dielectric properties used in this study, such as conductivity and relative permittivity, are taken from [14], which describes a method for creating realistic breast phantoms for the microwave detection of breast cancer. The breast model's skin has a radius of 30 mm and thickness of 4 mm. The fat has a 26 mm radius and a 5 mm thickness. Furthermore, the glandular radius is 21 mm. Figure 2 represents the breast model without any anomaly. A radius of 5 mm spherical malignant tumor placed in several positions of the human breast phantom model is shown in Figures 3(a), (b), (c), and (d). The coordinates x, y, and z for the tumor are: in the middle $(0, 0, -10)$, the right side $(0, 13.5, -8.5)$, and the left side $(0, -13.5, -8.5)$.

3. RESULTS AND DISCUSSION

After manufacturing the proposed antenna's prototype on the 1 mm thickness of the FR4 HTG-175 with LPKF Proto Mat S103, measurements have been made with a two-port ZVA50 VNA in the frequency range of 3.1–8.3 GHz. Table 2 defines the electric parameters of the breast model. The final radiating

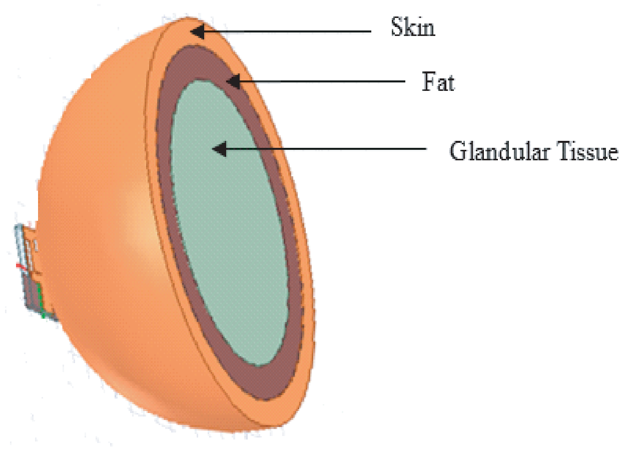

Figure 2. A designed model for a defective breast.

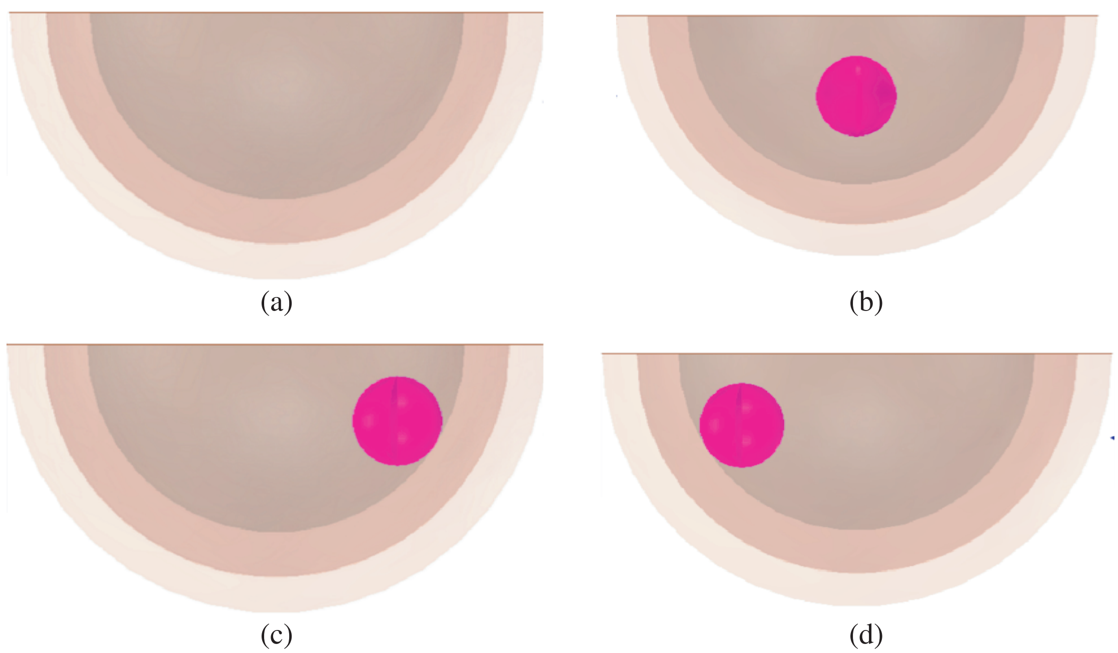

Figure 3. Breast model, (a) without tumor, (b) tumor in the middle, (c) tumor in the right-side, and (d) tumor on the left side.

Table 2. Different parameters for the breast model.

S. No.	Tissue	Relative permittivity	Conductivity (S/m)	Density (kg/m^2)
1	Skin	34	4.4	1100
2	Fat	14	0.9	920
3	Glandular	28	3.7	1050
4	Tumor	48	6.1	1070

(a) (b)

Figure 4. (a) The manufactured top view of the proposed breast cancer antenna. (b) The manufactured bottom view of the proposed breast cancer antenna.

element dimension is $12 \times 12 \times 1\,\mathrm{mm}^3$. The top and bottom views of the prototype, manufactured and tested, are shown in Figure 4.

3.1. Reflection Coefficient for the Design Stages

The reflection coefficient is an essential criterion to characterize the antenna, as the parameter performance is reduced after placing the antenna close to the breast. As a result, the reflection coefficient should be good enough. Therefore, this design aims to get a good antenna performance regarding the reflection coefficient within the ISM band. Further, in Figure 5, stages 4 and 5 show that importing slots and cuts in the design positively affected antenna characteristics regarding resonance frequency, bandwidth, and reflection coefficient.

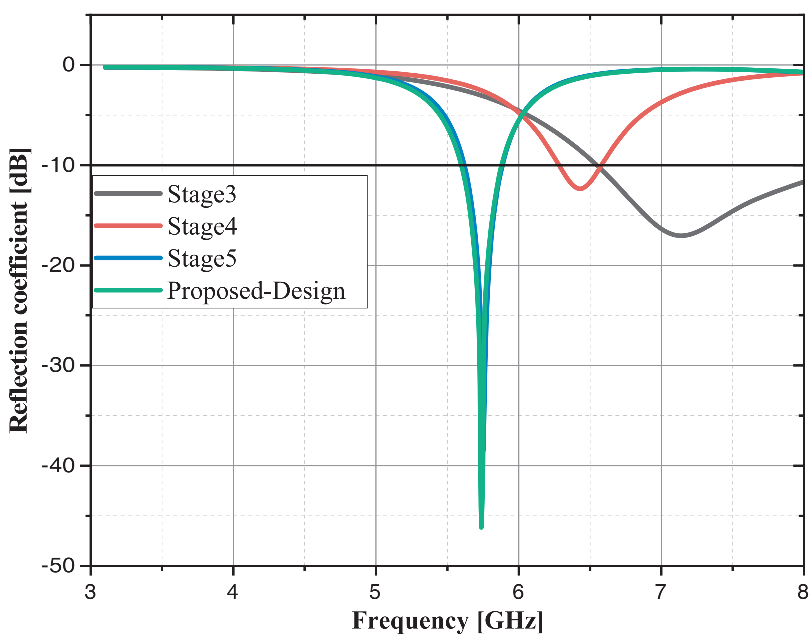

Figure 5. Reflection coefficient of the design stages.

3.2. Parametric Analysis

To optimize the antenna's performance, parameters $WS1$ and $LS1$ were optimized in stage 4 of the design. In addition, the length of the ground plane $Lg1$ was optimized to check the optimum value for the design.

3.2.1. Effect of Varying $WS1$

In stage 4, the parametric analysis in HFSS was performed, and the value of $WS1$ was increased by 0.5 from 0.5 mm to 2 mm. Figure 6(a) shows the influence on antenna parameters by varying $WS1$. Moreover, the bandwidth increases by reducing the value of $WS1$, but the reflection coefficient worsens. The bandwidth for 1 mm, 1.5 mm, and 2 mm is 301 MHz, 280 MHz, and 270 MHz, respectively.

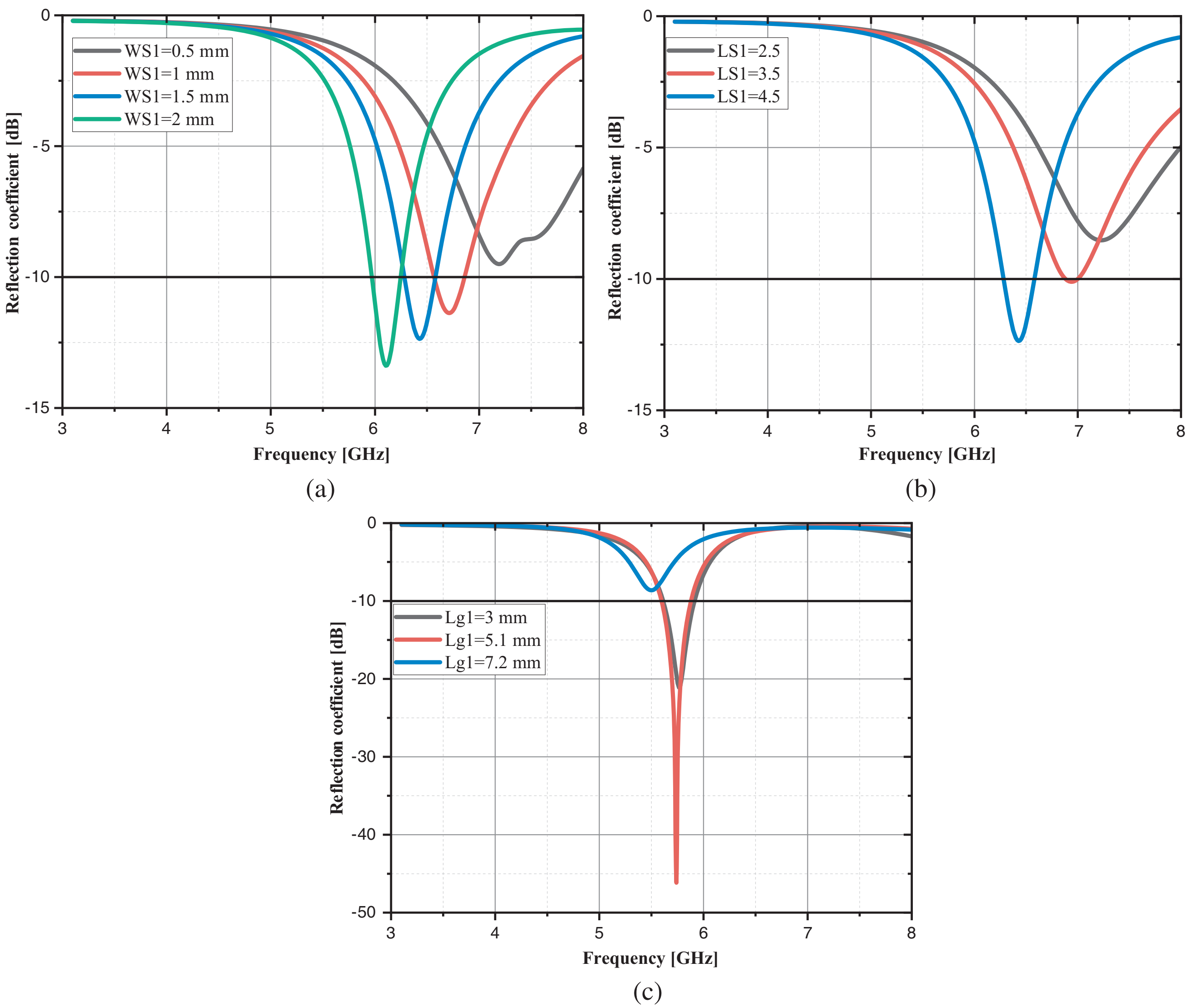

Figure 6. (a) Variation of $WS1$ parameter. (b) Variation of $LS1$ parameter. (c) Variation of $Lg1$ parameter.

3.2.2. Effect of Varying $LS1$

The influence of varying $LS1$ on antenna parameters is illustrated in Figure 6(b). The value of $LS1$ was increased by 1 mm from 2.5 to 4.5. As the value of $LS1$ increases, the reflection coefficient lowers, and the resonance frequency decreases.

3.2.3. Parametric Study of the Ground Plane Length

After getting the proposed design, it analyzed parameter $Lg1$ to find the best bandwidth and return loss value. $Lg1$ is the length of the ground plane, as seen in Figure 1(b). Hence, by varying $Lg1$ from 3 to 7.2 with a step of 2.1 mm, the optimum value was $Lg1 = 5.1$ mm, which gives better bandwidth and reflection coefficient results, as seen in Figure 6(c).

3.3. Simulated and Measurement of Reflection-Coefficient and VSWR

The proposed antenna has been prototyped, as depicted in Figure 4. A reflection coefficient of -51.22 dB at 5.73 GHz was obtained during the experimental validation process, while the simulated one got to -46.16 dB at 5.74 GHz. The two results are close and plotted in Figures 7(a) and (b).

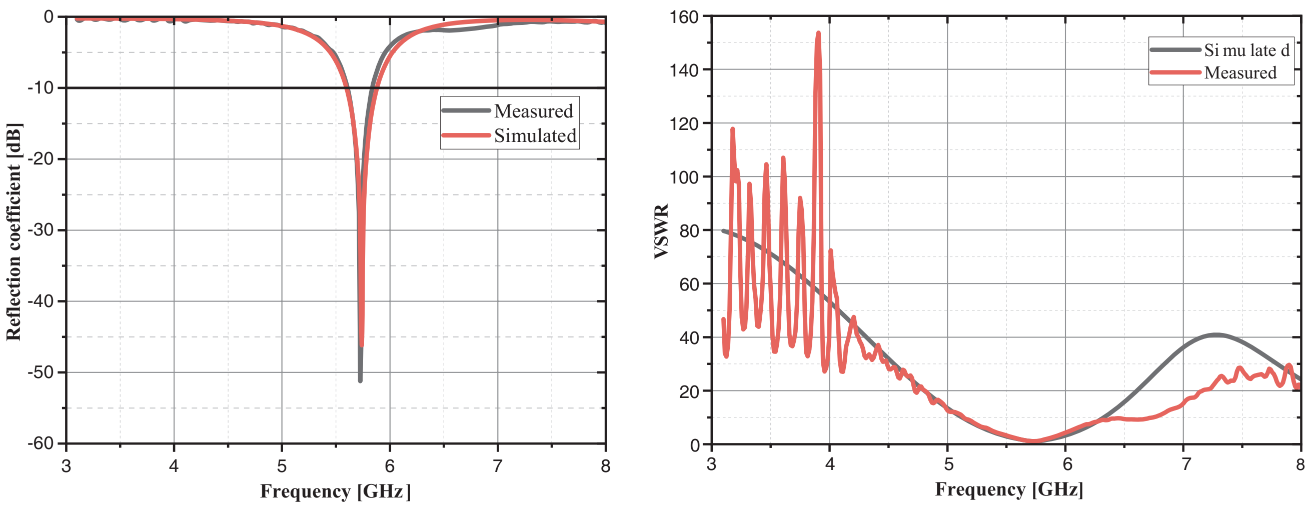

(a) (b)

Figure 7. (a) The Reflection-coefficient at the operating frequency. (b) The voltage standing wave ratio of the proposed antenna.

The measured values are so low that they make it a selective radiation antenna. The simulated and measured devices cover 5.6–5.88 GHz and 5.6–5.83 GHz, respectively. That represents 280 MHz and 230 MHz of bandwidth each. As a consequence, the radiation device is narrowband.

The antenna size reduction has been evaluated using an approach that compares the active patch area of a typical microstrip antenna A_r to to the proposed antenna A_p when it resonates at the same frequency as that given in Eq. (5) [15]

$$M(\%) = \left[\frac{A_r(f_r)|_{f_r=f_0} - A_p(f_r)|_{f_r=f_0}}{A_r(f_r)|_{f_r=f_0}}\right] 100 \tag{5}$$

where A_r is the active patch area of a microstrip antenna resonating at the same frequency. The suggested antenna has an active area of A_p. A rectangular microstrip resonating at 5.7 GHz has an active patch area of 401.70 mm^2 (18.256 $\times$ 22.004 mm^2). Using Eq. (5) and comparing the antenna with a typical microstrip antenna yields an active patch size reduction of 64.15%. Hence, this designed antenna might be classified as a miniaturized radiating device. Also, it is observed that for both simulated and measured radiating elements, the voltage standing wave ratio (VSWR) is around 1.01

at the resonance frequency, as depicted in Figure 7(a). Therefore, according to [16, 17], the proposed antenna matches well with the feedline. This indicates that a maximum incident power is transferred to the radiating element, which results in 82% radiating efficiency at 5.74 GHz.

3.4. Current Distribution

Figure 8 depicts the current distribution at the resonance frequency (5.73 GHz) and the current flow with a specific energy in different antenna compartments.

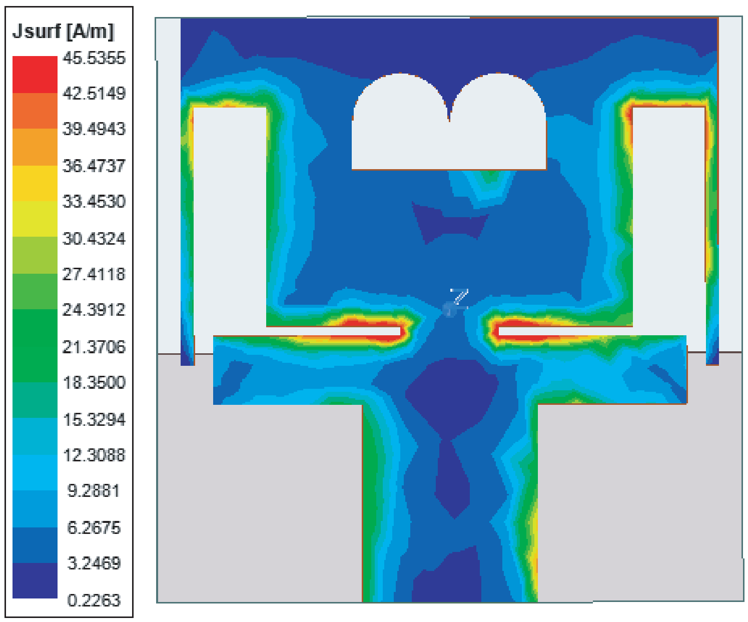

Figure 8. The current distribution of the proposed antenna.

As seen in Figure 8, the current is distributed more at the edges of the radiating element and less inside the antenna. This behavior is normal and conforms to the approach presented in [16].

3.5. Gain and Radiation Pattern

The antenna gain is selected from the two-antenna transmission methods based on the Friis telecommunication equation as given below,

$$|S_{21}|^2 = G_t G_r \left(\frac{c}{4\pi d f_0}\right)^2 \tag{6}$$

where S_{21} is the transmission coefficient, f_0 the operating frequency, d the distance between both antennas, c the free space speed, and G_t and G_r are the transmitter and receiver antenna gains, respectively. Using the Friis equation for two identical antennas ($G_r = G_t$), Eq. (6) becomes [16, 17] as follows,

$$G_t^{\mathrm{dBi}} = \frac{1}{2}\left[S_{21}^{\mathrm{dB}} + 32.5 + 20\log\left(f_{0_{(\mathrm{GHz})}}\right) + 20\log(d_m)\right] \tag{7}$$

Using Eq. (7) derived from Eq. (6), two similar antennas placed 10 cm from each other allow measuring a gain of 2.9 dBi at 5.7 GHz, as seen in Figure 9. The resonance frequency moves slightly in the presence of the second radiating device, but the bandwidth is the same.

Figure 10 shows the experimental bench measurement, where two identical antennas are connected to both VNA ports to measure the transmission coefficient (S_{21}). That coefficient is essential in the Friis equation to get the antenna's gain parameter.

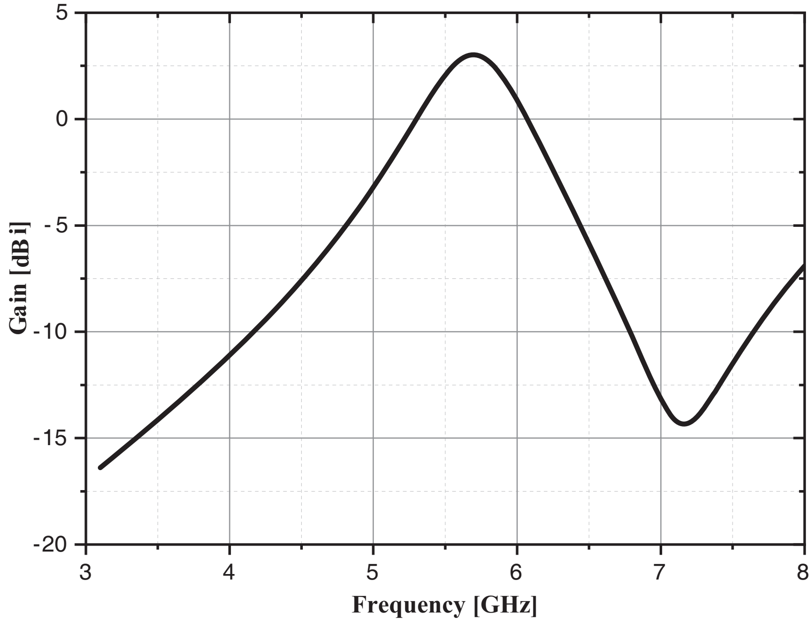

Figure 9. Gain versus frequency when using the Friis equation.

A controlled distance separating two antennas (transmitter and receiver) and a scanned operating frequency help determine the gain. The antennas receive the electromagnetic signal through the RF cable linked to the VNA. Figure 10 shows that a printed SMA connector connects that RF cable and the antenna. When an antenna is miniaturized and its ground plane defective, its gain, radiation efficiency, bandwidth, and polarization are all impacted [16]. The miniaturization of its dimensions and the DGS lead to low antenna gain. Hence, the proposed design employs a partial ground structure, which leads

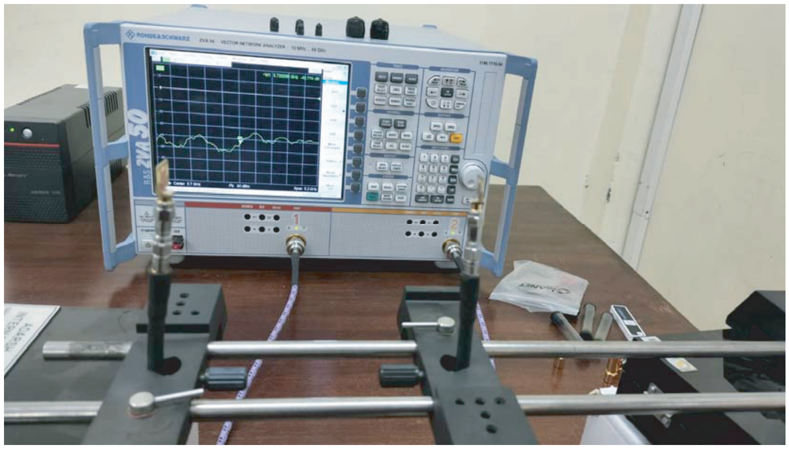

Figure 10. Radio frequency bench for the measurement of the antenna's gain.

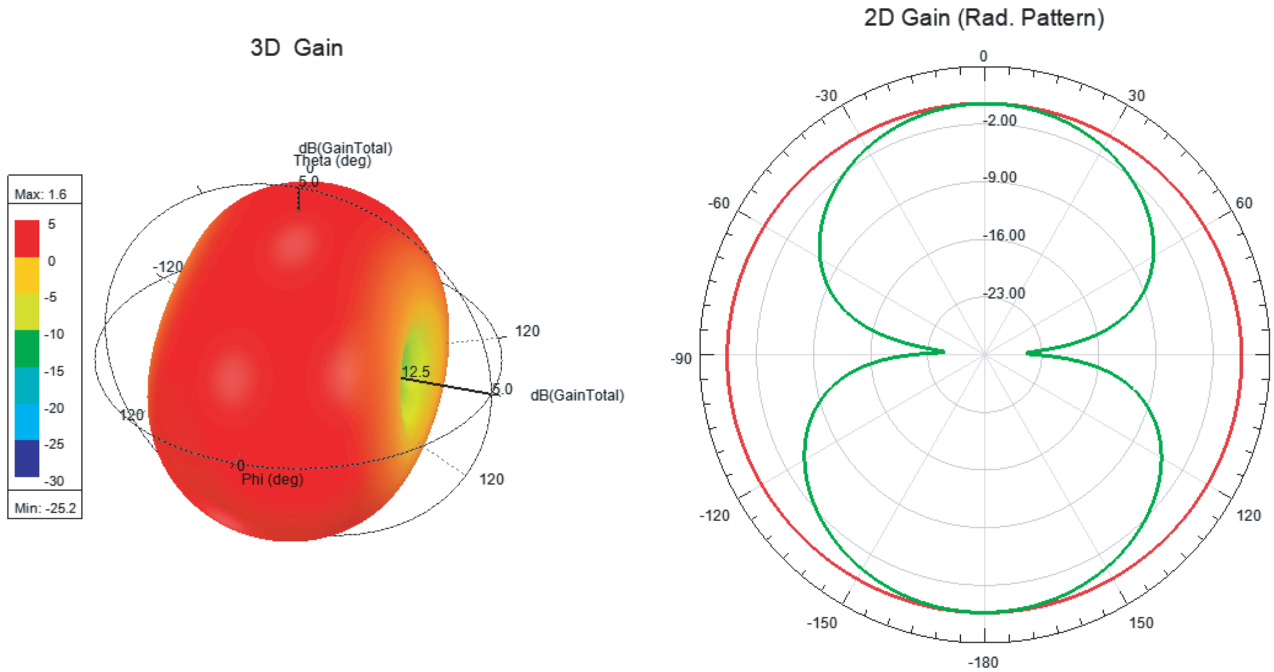

(a) (b)

Figure 11. (a) Gain of the Proposed antenna. (b) The proposed antenna's radiation pattern.

to a low radiated power and a low gain at the operating frequency. A 360° coil with fixed pitch allows the coil to describe a trajectory, as presented in Figure 11(a). Figure 11(b) shows an omnidirectional radiation pattern on the E-plane and a bi-directional radiation-pattern on the H plane.

It is preferable for antenna Microwave Imaging for BCD to have a high gain and directional radiation pattern because it can help minimize the environment noise effect and increase the signal penetrating the human target area. However, the main challenges in designing the proposed antennas are related to the physical size to allow many antennas to collect more information on the scattering signal for a high-quality image reconstruction [18].

4. IMPACT OF THE BREAST WITH AND WITHOUT TUMOR

The reflection coefficient, resonance frequency, VSWR, and maximum electric fields are the parameters that have particular attention in this section through the tumor breast impact. In addition, to ensure the antenna's capability, the tumor is placed in several areas on the phantom breast model. Also, three ways are suggested to study the impact of the tumor through the antenna: the antenna is used on the breast; both antennas are on the same breast; the breast is between two antennas while the antennas are in a distance of 100 mm away from each other.

4.1. Antenna on the Breast

In this case, it is supposed that one antenna is placed on the breast, as shown in Figure 12(a). In that case, the reflection coefficient is presented in Figure 12(b).

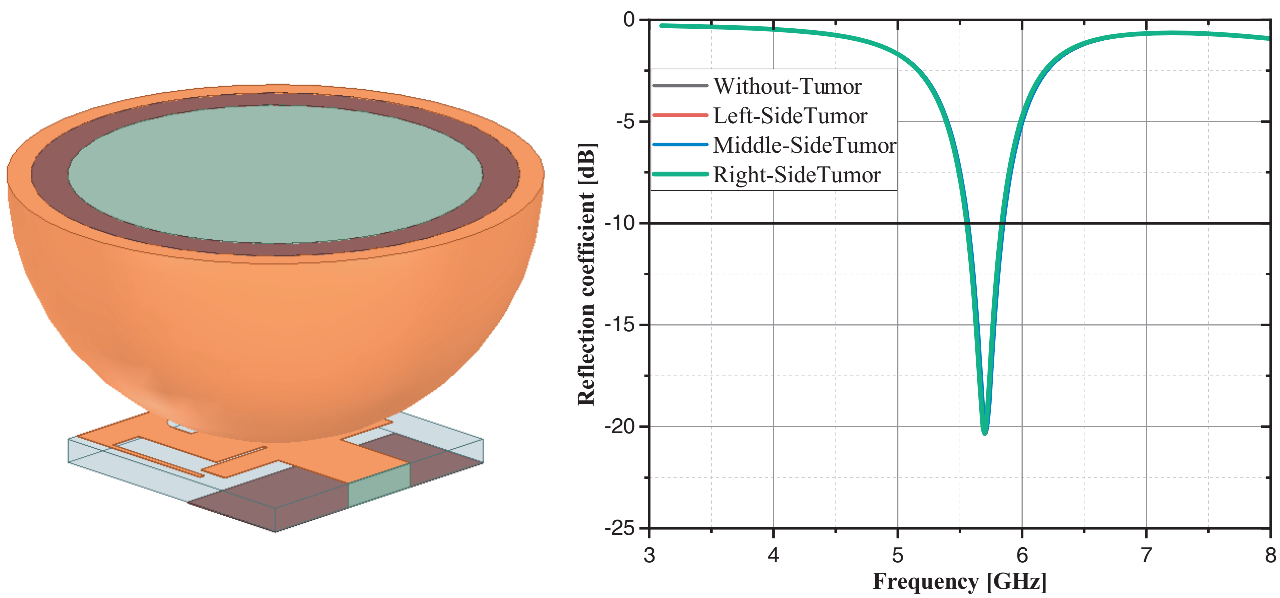

(a) (b)

Figure 12. (a) An antenna on the breast Phantom. (b) Antenna Reflection-coefficient in different tumor positions.

Regarding the position of the tumor on the breast, the reflection coefficient changes in its matching level parameter. In the absence of a tumor, the reflection coefficient was -19.86 dB, but once the tumor is placed on its left, right, or middle sides, it becomes -20.348 dB, -20.234 dB, and -20.225 dB, respectively. Moreover, a slight slip of the resonance frequency is noticed for the middle side case. Meanwhile, the VSWR in the perfect case is 1.226. But when the tumors are on the breast's left, right, and middle sides, VSWR becomes 1.21, 1.23, and 1.24, respectively. It is observed that the presence of the breast model increases the VSWR values.

Table 3. Comparison of breast tumor impact on the antenna's reflection coefficient.

	Reflection coefficient (dB)	Resonance frequency (GHz)
Breast without tumor	-19.86	5.700
Breast with left-side tumor	-20.348	5.700
Breast with right-side tumor	-20.233	5.700
Breast with middle-side tumor	-20.225	5.713

Table 4. Maximum electric and magnetic fields from the healthy and affected breast.

Magnitude E, Magnitude H	Without tumor	Left-tumor	Right-tumor	Middle
Maximum Electric field (V/m)	299460	469370	319200	521220
Maximum Magnitude field (A/m)	117.95	121.203	138.486	101.160

As Table 3 shows, Table 4 confirms the tendency of the tumor's presence according to the breast's position. The tumor breast position increases the electric and magnetic fields, except for the middle position on the magnetic field, which decreases.

4.2. Antennas on the Breast

In this case, it is supposed that both antennas (transmitter and receiver) are on the same breast. Only one is on the affected area, as shown in Figure 13. The transmitter antenna's reflection coefficient in different tumor positions is plotted in Figure 14. At the same time, a comparison of the healthy and tumors breasts in some positions is presented in Table 5 through their reflection coefficientd and resonance frequencies.

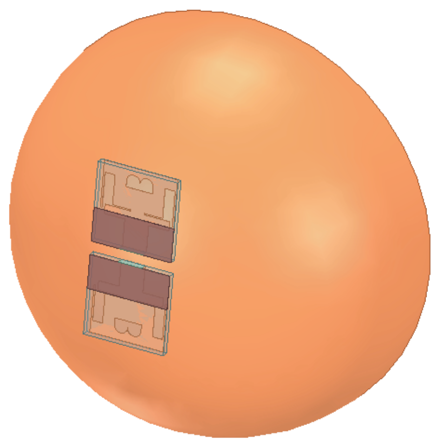

Figure 13. Two antennas on the breast phantom.

Table 5. Comparison of breast tumor impact when using two antennas on the breast phantom.

	Reflection coefficient (dB)	Resonance frequency (GHz)
Breast without tumor	-15.38	5.778
Breast with left-side tumor	-15.74	5.752
Breast with right-side tumor	-15.60	5.739
Breast with middle-side tumor	-15.81	5.752

In the absence of a tumor, the reflection coefficient is -15.385 dB at 5.778 GHz, but with the tumor on the left, right, and middle sides, the reflection coefficient is -15.740 dB, -15.602 dB, and -15.81 dB at the frequencies 5.752 GHz, 5.739 GHz, and 5.752 GHz, respectively. Hence, the antenna provides lower values of S-parameters and lower resonance frequencies in the presence of a malignant tumor. Moreover, the detection will be better when using two antennas on the breast phantom.

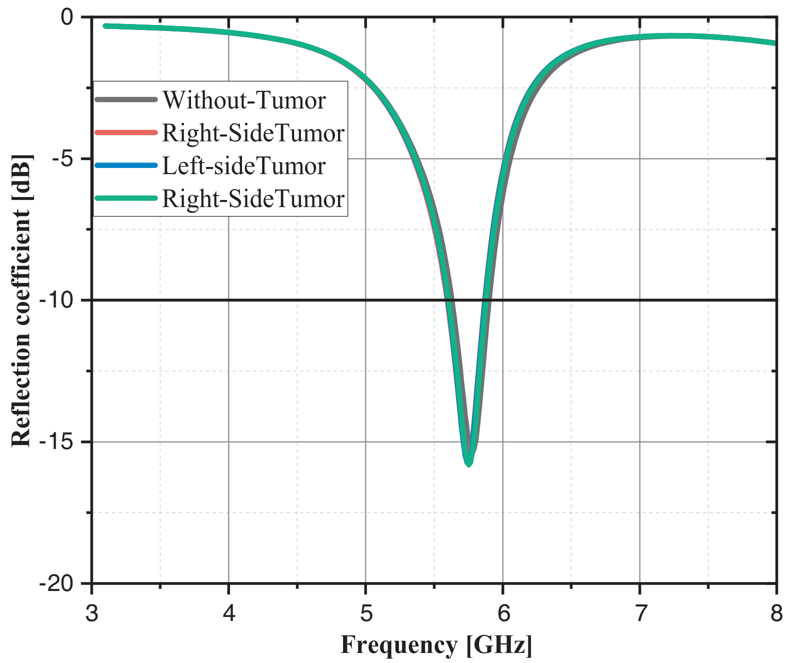

Figure 14. Reflection coefficient when using two antennas on the breast.

4.3. Breast between Two Antennas

In such a situation, the breast is placed between two antennas. Therefore, the two antennas have 10 cm gap from each other. Figure 15 depicts a breast model position between two antennas, where one is placed on the breast and the other with a distance away from it.

Figure 15. Breast between two antennas 10 cm far from each other.

Figure 16 represents the reflection coefficient when two antennas are used with a gap between them. It is noticed that putting the antennas away from the breast lowers the reflection coefficient, whereas antennas on the breast affect the performance of the reflection coefficient. In both situations, the resonance frequency is reduced in the presence of a malignant tumor.

The model can detect a small tumor in 5 mm at three different positions, namely right, middle, and left, as noticed. Moreover, using more antennas around the breast will enhance the detection of breast cancer. The measurements at different positions (different angles or depths within the breast) ensure a robust detection algorithm to detect tumors in various locations. In addition, this could include testing the algorithm on a range of breast tissue samples, including samples from women with different breast types.

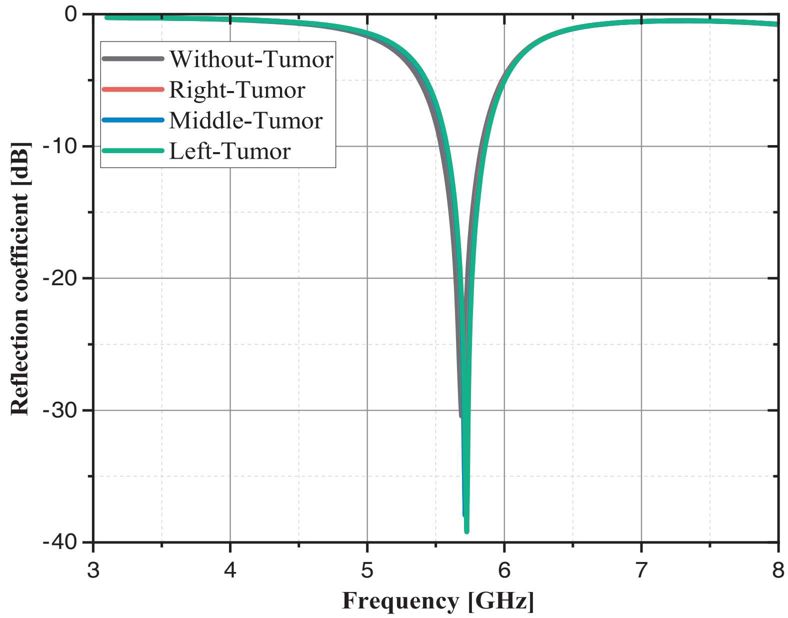

Figure 16. Antennas reflection coefficient in different positions.

Table 6 summarizes the two antennas placed on the same breast. Putting two similar antennas between the breasts 10 cm from each other, one is near the affected area, and the other is far away, as shown in Figure 15. Again, it is seen that the antenna provides lower values of S_{11} parameters in the presence of the tumor. In addition, it is also seen that using two antennas with a gap between them enhances the difference between the healthy breast and affected breast regarding the reflection coefficient, which can lead to better detection. Using a narrow bandwidth antenna for imaging diagnostic may not provide the necessary resolution and accuracy for detailed tumor imaging. Ultra-Wideband (UWB) antennas are often used in microwave imaging for cancer detection because they can provide high-resolution and accurate images. However, the proposed antenna in the ISM band can give a low penetration. The signal processing algorithm used in qualitative microwave imaging to improve the detection of breast cancer in narrow bandwidth consists of five steps. First, microwave signals are transmitted into the breast tissue, and the reflected signals are received and recorded in the data acquisition step. The acquired signals are then preprocessed to remove noise and corrected for any distortions to ensure that the data is suitable for further analysis. Next, in the feature extraction step, relevant features such as the signals' amplitude, phase, or frequency are extracted to create images of the tissue and identify abnormalities. The extracted features are then used to reconstruct an image of the breast tissue through techniques such as inverse scattering, tomography, or back projection in the image reconstruction step. Finally, the reconstructed image is interpreted by a radiologist or medical professional to identify tumors or other abnormalities in the image interpretation step. It is possible

Table 6. Comparison of breast tumor impact when using two antennas on the breast phantom 100 mm for each other.

	Reflection coefficient (dB)	Resonance frequency (GHz)
Breast without tumor	−30.430	5.687
Breast with left-side tumor	−39.204	5.726
Breast with right-side tumor	−37.571	5.713
Breast with middle-side tumor	−37.948	5.713

to use a narrow bandwidth antenna and other techniques to achieve detailed tumor imaging. For example, using synthetic aperture radar (SAR) imaging improves the resolution of a narrow bandwidth antenna. SAR imaging generally uses a moving antenna to transmit microwave pulse signals to the target and collect the reflected echoes [19]. The echoes collected from the target are processed using signal-processing algorithms to form an image of the target. The image is then analyzed to extract information about the target, including any abnormal scattering patterns that may indicate the presence of breast cancer. In addition, by enhancing the image's resolution, the signal processing algorithm can help identify small tumors, making SAR imaging a helpful tool for early breast cancer detection. The back-projection (BP) is one of the most used algorithms for SAR image formation due to its robustness and quality of results [20]. In addition, Fourier-based image reconstruction methods can be an excellent solution to decrease the computational cost in SAR microwave imaging systems. These methods use mathematical techniques such as the Fast Fourier Transform to process the radar data and reduce the computational cost efficiently [21, 22]. Another concrete method is frequency-modulated continuous-wave (FMCW) radar imaging, which uses a continuous-wave radar signal with a frequency modulated over time to obtain the image. By analyzing the echoes of the modulated signal, the object's relative permittivity and conductivity can be determined, which can be used to identify different types of tissue [23].

5. COMPARATIVE STUDY

Some latest studies have been compared in Table 7 with the proposed, designed antenna.

Table 7. A comparative study with the latest works.

Ref.	Bandwidth (GHz)	Radiation efficiency (%)	Size (mm^2)	Reflection coefficient (dB)	Gain (dB)	Application
[12]	1.5–3	None	77×60.46	-37.27	None	MWI
[24]	2–5	None	50×40	< -10	5.5	MWI
[25]	0.9–9.6	None	16×16	< -10	None	MWI
[26]	3.7–5.7	86	32×32	-25	2.00	MWI
[27]	1.6–10	None	60×70	< -10	4.431	MWI
[28]	3.4–10	96.98	18×28	< -10	3.95	MWI
[29]	2–12	None	45×31	< -10	5.00	WWT
This work	5.72–5.82	82	12×12	-46.15	2.9	MWI

where wideband wireless technology (WWT) and MWI are different applied technologies. The comparison study presented in Table 7 shows that the proposed antenna is among the best-matched planar antenna. With a return loss of 46.15 dB, the characteristic antenna impedance is 50.495 Ω. Therefore, the proposed planar antenna is well adapted. At the same time, the suggested planar antenna is selective with the ISM band compared to the other studies. The DGS technique sometimes limits the antenna gain to minus values, as in this antenna which achieved 2.9 dB. This is caused by a poor electrical field distribution between the ground and the radiation element [15].

Regarding the component (radiation element) integration, the proposed antenna design is smaller than all cited in Table 7. Hence, this structure is easy to integrate into a space-constrained environment. Furthermore, the proposed antenna can be considered a tiny chip on the patient's body. Therefore, it will not hinder movements.

6. CONCLUSIONS

This research presents a new small-size microstrip patch antenna for breast cancer detection in the ISM band of 5.72–5.82 GHz. The antenna was simulated in Ansys HFSS software and manufactured using LPKF Proto Mat S103. The measurement was completed using a two-port ZVA50 VNA. The antenna has a good return loss with the VSWR below 2 at the resonance frequency. Hence, the simulated and measured results demonstrate that the proposed antenna is a promising candidate for breast cancer detection. The antenna was tested on a simulated breast phantom cancer-free and with a small tumor in different positions to check the device's capability. The presence of the tumor in the breast can be detected by observing the antenna parameters such as reflection coefficient and VSWR. This work investigated the reflection coefficient parameter to detect breast cancer in different positions using three scenarios: an antenna on the breast model, two antennas on the breast model, and a breast model between two antennas with a 10 cm gap. The best scenario, which gives more contrast between healthy and affected breasts, was the last study done. Furthermore, the reflection coefficient values are an essential indicator for cancer identification because they are significantly lowered in the presence of a tumor in different positions. Moreover, the small physical size of the proposed design allows a huge number of them to be used on the breast area, giving more contrast between healthy and cancer breasts regarding antenna parameters. Due to the Lab equipment, this suggested antenna has not been concerned with clinical experiments but could be used to explore.

ACKNOWLEDGMENT

The authors thank the reviewers for the time and effort they devoted to improving this work's quality through their comments and suggestions. In addition, they appreciate the Pan African University, Institute for Basic Science, Technology, and Innovation, and Jomo Kenyatta University of Agricultural and Technology for technical support.

REFERENCES

1. Sugitani, T., S. Kubota, S. Kuroki, et al., "Complex permittivities of breast tumor tissues obtained from cancer surgeries," *Appl. Phys. Lett.*, Vol. 104, No. 25, Jun. 2014.
2. Fear, E. C., "Microwave imaging of the breast," *Technol. Cancer Res. Treat.*, Vol. 4, No. 1, 69–82, Jun. 2005.
3. Sarestoniemi, M., J. Reponen, M. Sonkki, et al., "Breast cancer detection feasibility with UWB flexible antennas on wearable monitoring vest," *2022 IEEE Int. Conf. Pervasive Comput. Commun., Work. other Affil. Events, PerCom Work. 2022*, 751–756, 2022, doi: 10.1109/PerComWorkshops53856.2022.9767512.
4. Srinivasan, D. and M. Gopalakrishnan, "Breast cancer detection using adaptable textile antenna design," *J. Med. Syst.*, Vol. 43, No. 6, 1–10, 2019.
5. Bhavani, S., "Wearable microstrip circular patch antenna for breast cancer detection," *IEEE International Symposium on Antennas and Propagation and USNC-URSI*, 1273–1274, 2021, doi: 10.1109/APS/URSI47566.2021.9704255.
6. Bohra, S. and T. Shaikh, "UWB microstrip patch antenna for breast," *Int. J. Adv. Res. Electron. Commun. Eng.*, Vol. 5, No. 1, 1–13, 2016.
7. Gupta, N. P., P. K. Malik, and B. S. Ram, "A review on methods and systems for early breast cancer detection," *Proc. Int. Conf. Comput. Autom. Knowl. Manag. ICCAKM 2020*, 42–46, Jan. 2020.
8. Rao, P. K. and R. Mishra, "Ultra-wide-band flexible antenna for breast cancer detection," *2019 IEEE 5th Int. Conf. Converg. Technol. I2CT 2019*, Vol. 5880, 5–8, 2019.
9. Kumar, V., H. V. Kumar, and T. S. Nagaveni, "Design of microstrip patch antenna to detect breast cancer analysis of hyperspectral images view project design of microstrip patch antenna to detect breast cancer," *Artic. ICTACT J. Microelectron.*, 1, 2020.

10. Ouerghi, K., N. Fadlallah, A. Smida, R. Ghayoula, J. Fattahi, and N. Boulejfen, "Circular antenna array design for breast cancer detection," *2017 Sensors Networks Smart Emerg. Technol. SENSET 2017*, Vol. 2017-Janua, 1–4, Nov. 2017.
11. Mansoor, F., T. Tan, and S. I. Latif, "The performance of an ultra-wideband elliptical ring monopole antenna with a humanoid breast phantom," *2017 IEEE Antennas Propag. Soc. Int. Symp. Proc.*, Vol. 2017-Janua, 105–106, 2017.
12. Islam, R., F. Mahbub, S. Abdul Kadir Al-Nahiun, S. Banerjee Akash, R. Rashidul Hasan, and M. Abdur Rahman, "Design of an on-body rectangular microstrip patch antenna for the diagnosis of breast cancer using S-band," *Lect. Notes Networks Syst.*, Vol. 216, 1033–1044, 2022.
13. Sinha, S., T. S. R. Niloy, R. R. Hasan, M. A. Rahman, and S. Rahman, "A wearable microstrip patch antenna for detecting brain tumor," *Proc. Int. Conf. Comput. Autom. Knowl. Manag. ICCAKM 2020*, 85–89, Jan. 2020.
14. Porter, E., J. Fakhoury, R. Oprisor, M. Coates, and M. Popovic, "Improved tissue phantoms for experimental validation of microwave breast cancer detection," *EuCAP 2010 — 4th Eur. Conf. Antennas Propag.*, 2–7, 2010.
15. Moukala Mpele, P., F. Moukanda Mbango, D. B. O. Konditi, and F. Ndagijimana, "A novel quadband ultra miniaturized planar antenna with metallic vias and defected ground structure for portable devices," *Heliyon*, Vol. 7, No. 3, e06373, 2021.
16. Moukala Mpele, P., F. Moukanda Mbango, D. B. O. Konditi, and F. Ndagijimana, "A tri-band and miniaturized planar antenna based on countersink and defected ground structure techniques," *Int. J. RF Microw. Comput. Eng.*, Vol. 31, No. 5, 1–12, 2021.
17. Bamy, C. L., F. Moukanda Mbango, D. B. O. Konditi, and P. Moukala Mpele, "A compact dual-band Dolly-shaped antenna with parasitic elements for automotive radar and 5G applications," *Heliyon*, Vol. 7, No. 4, e06793, 2021.
18. Borja, B., J. A. Tirado, and H. Jardón, "An overview of UWB antennas for microwave imaging systems for cancer detection purposes," *Progress In Electromagnetics Research B*, Vol. 80, 173–198, 2018.
19. Liu, H., X. Shang, and X. Ye, "Breast cancer detection using synthetic aperture radar imaging and distorted born iterative method," *2018 Int. Appl. Comput. Electromagn. Soc. Symp. China, ACES-China 2018*, 1–2, 2019.
20. Doerry, A., "Basics of polar-format algorithm for processing synthetic aperture radar images," *Sandia Natl. Lab. Rep. SAND2012-3369*, May 2012, [Online], available: http://www.academia.edu/download/30537796/PFA_SANDIA.pdf.
21. Abbasi, M., A. Shayei, M. Shabany, and Z. Kavehvash, "Fast Fourier-based implementation of synthetic aperture radar algorithm for multistatic imaging system," *IEEE Trans. Instrum. Meas.*, Vol. 68, No. 9, 3339–3349, 2019.
22. Oloumi, D., R. S. C. Winter, A. Kordzadeh, P. Boulanger, and K. Rambabu, "Microwave imaging of breast tumor using time-domain UWB circular-SAR technique," *IEEE Trans. Med. Imaging*, Vol. 39, No. 4, 934–943, 2020.
23. Pisa, S., E. Pittella, and E. Piuzzi, "A survey of radar systems for medical applications," *IEEE Aerosp. Electron. Syst. Mag.*, Vol. 31, No. 11, 64–81, 2016.
24. Syed, A., M. Sheikh, M. T. Islam, and H. Rmili, "Metamaterial-loaded 16-printed log periodic antenna array for microwave imaging of breast tumor detection," *Int. J. Antennas Propag.*, Vol. 2022, 2022.
25. Salimitorkamani, M., M. Mehranpour, and H. Odabasi, "A compact ultrawideband slotted patch antenna for early stage breast tumor detection applications," *Int. J. Microw. Wirel. Technol.*, 1–9, 2022.
26. Slimi, M., B. Jmai, H. Dinis, and A. Gharsallah, "Microwave imaging for breast tumor detection using a CPW antenna," *Indian J. Sci. Technol.*, Vol. 15, No. 13, 554–560, 2022.
27. AlOmairi A. and D. Ç. Atilla, "Ultra-wide-band microstrip patch antenna design for breast cancer detection," *Electrica*, Vol. 22, No. 1, 41–51, Dec. 2021.

28. Ponnapalli, V. L. N. P., S. Karthikeyan, and J. L. Narayana, "A circular slotted shaped UWB monopole antenna for breast cancer detection," Vol. 104, 57–65, 2022.
29. Serria, E. A. and M. I. Hussein, "Implications of metamaterial on ultra-wide band microstrip antenna performance," *Crystals*, Vol. 10, No. 8, 1–24, 2020.